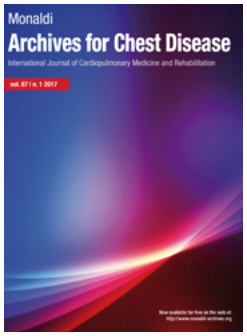

Monaldi Archives for Chest Disease

eISSN 2532-5264 https://www.monaldi-archives.org/

Publisher's Disclaimer. E-publishing ahead of print is increasingly important for the rapid dissemination of science. The ***Early Access*** service lets users access peer-reviewed articles well before print / regular issue publication, significantly reducing the time it takes for critical findings to reach the research community.
These articles are searchable and citable by their DOI (Digital Object Identifier).

The **Monaldi Archives for Chest Disease** is, therefore, e-publishing PDF files of an early version of manuscripts that have undergone a regular peer review and have been accepted for publication, but have not been through the typesetting, pagination and proofreading processes, which may lead to differences between this version and the final one.
The final version of the manuscript will then appear in a regular issue of the journal.

E-publishing of this PDF file has been approved by the authors.

All legal disclaimers applicable to the journal apply to this production process as well.

Monaldi Arch Chest Dis 2023 [Online ahead of print]

To cite this Article:
Alamro B, Pergola V, Eltayeb A, et al. **Role of three-dimensional transesophageal echocardiography in cardiac myxomas: an imaging challenge.** *Monaldi Arch Chest Dis* doi: 10.4081/monaldi.2023.2768

©The Author(s), 2023
Licensee PAGEPress, Italy

Note: The publisher is not responsible for the content or functionality of any supporting information supplied by the authors. Any queries should be directed to the corresponding author for the article.

All claims expressed in this article are solely those of the authors and do not necessarily represent those of their affiliated organizations, or those of the publisher, the editors and the reviewers. Any product that may be evaluated in this article or claim that may be made by its manufacturer is not guaranteed or endorsed by the publisher.

Role of three-dimensional transesophageal echocardiography in cardiac myxomas: an imaging challenge

Bandar Alamro,[1,2] Valeria Pergola,[3] Abdalla Eltayeb,[1,4] Amal Alshammari,[1] Naji Kholaif,[1,2] Ahmad Alhamshari,[2] Mohammed Al Admawi,[1] Shamayel Mohammed,[1] Feras Khaliel,[1] Domenico Galzerano[1,2]

[1]The Heart Centre, King Faisal Specialist Hospital and Research Center, Riyadh, Saudi Arabia
[2]College of Medicine, Alfaisal University, Riyadh, Saudi Arabia
[3]Department of Cardio-Thoraco-Vascular Sciences and Public Health, University of Padua, Italy
[4]Division of Cardiovascular Medicine, Krannert Cardiovascular Institute, Indiana University School of Medicine, Indianapolis, IN, USA

Corresponding author: Abdalla Eltayeb, The Heart Centre, King Faisal Specialist Hospital and Research Center, Riyadh, Saudi Arabia. E-mail: abdullaheltayeb2002@gmail.com

Contributions: All the authors made a substantive intellectual contribution, performed part of the experiments. All the authors read and approved the final version of the manuscript and agreed to be accountable for all aspects of the work.

Conflict of interest: The authors declare that they have no competing interests, and all authors confirm accuracy.

Ethics approval: This study project has been conducted in accordance with the ethical principles contained in the Declaration of Helsinki (2000), the ICH Harmonized Tripartite Good Clinical Practice Guidelines, the policies and guidelines of the Research Advisory Council (RAC) of the King Faisal Specialist Hospital and Research Center, and the laws of Saudi Arabia. As this was a retrospective study and did not involve any direct contact with patients or their families and does not pose more than a minimal risk to patients a waiver of informed consent was approved by RAC.

Availability of data and materials: The datasets used and/or analyzed during the current study are available from the corresponding author on reasonable request.

Abstract

Nowadays, the diagnosis of cardiac myxomas (CM), particularly the histological types, remains a challenge. Two-dimensional (2D) transthoracic (TT) and transesophageal (TEE) echocardiography (ECHO) represent the first steps in the imaging pathway. 3D ECHO, implemented in imaging practice, appears to be an emerging diagnostic technique that overcomes some of the limitations of 2D ECHO while integrating the information provided by

magnetic resonance (MRI). However, its role in the imaging arena is still debatable. Analyzing 17 myxomas in 13 patients, the study uncovers a diverse anatomical spectrum. Classical CM morphology is a minority, with most myxomas being sessile and originating from unexpected locations (right ventricular outflow tract and left atrial appendage). Texture and size variations are also noted. Comparing imaging, 2D TEE outperforms 2D TT in visualizing anatomical features, especially attachment types. 3D TEE confirms 2D TT findings and offers more detailed assessments, identifying peduncles missed in four cases by 2D TEE. Two small recurrent myxomas were exclusively detected by 3D TEE, not by 2D TEE or MRI. Two patients have papillary myxomas, one has an embolism. Another patient with a solid myxoma also suffers an embolism, with a clot found at the apex during surgery. Our study showed that CM has a wide anatomical spectrum beyond the typical features, making the diagnosis challenging. Therefore, a multimodality imaging approach is essential for distinguishing CM from other cardiac masses and differentiating myxoma histological types. These findings stress the importance of incorporating 3D ECHO alongside other imaging techniques for a comprehensive evaluation.

Key words: cardiac myxomas; transesophageal echocardiography; 3-dimensional echocardiography; magnetic resonance imaging.

Introduction

Nowadays, the diagnosis of cardiac myxomas (CM), particularly of the histological types, remains a challenge [1-7]. Two-dimensional (2D) transthoracic (TT) and transesophageal (TE) echocardiography (ECHO) represent the first steps in the imaging pathway [5,8,9]. Even though echo has an excellent sensitivity for CM diagnosis however the specificity is still modest due to a wide differential diagnosis [1-9]. In the imaging scenario, three-dimensional (3D) TE ECHO, thanks to technological advances allowing fast reconstruction of realistic anatomic images of cardiac structure, has been implemented in routine imaging practice [10-12]. Currently, both transthoracic echocardiography and transesophageal echocardiography transducers can generate 3D images. However, 3D TE ECHO, which provides images of higher quality compared to 3D TT ECHO, is the modality capable of allowing for detailed anatomical imaging [10,11]. In the cardiac tumor imaging scenario, it appears to be an emerging diagnostic technique that overcomes some of the limitations of 2D ECHO while integrating the

information provided by magnetic resonance imaging (MRI) and cardiac computed tomography (CT) [12-21]. However, its role in the imaging arena is still debatable.

In the imaging pathway of cardiac masses and myxomas, the type and site of attachment (pedunculated or sessile), surface characteristics (smooth and bosselated versus irregular and fimbriated), and echotexture (presence of hemorrhagic areas and calcification showing different echotextures, homogeneous *versus* heterogeneous/non-homogeneous) hold paramount importance [5,8,9,12,21]. The correct visualization of these morphological features can lead to the diagnosis of the presence of myxomas versus other intracardiac masses, as well as the specific type of myxoma (solid or polypoid versus papillary or myxoid). Two types of myxomas in macroscopic examination have been identified: solid or polypoid myxomas with a round shape and a smooth surface usually attached to the interatrial septum (IAS) and papillary myxomas characterized by an asymmetrical and soft shape with an irregular surface attached to various locations. The latter type has been shown to have a higher risk of systemic embolism, either due to the irregular or friable villous surface of the tumor or through thrombus formation. However, thrombus formation may also be present in the solid type [1-7].

The majority of cardiac myxomas (CM) are polypoid and pedunculated (rarely sessile), presenting as round or ovoid tumors with smooth, glistening, or slightly lobulated surfaces, and a short broad base. Polypoid myxomas are typically compact, solid tumors with little tendency for spontaneous fragmentation. Less commonly detected are papillary myxomas, which exhibit multiple thinner or thicker villous, finger-like extensions and possess a soft, gelatinous structure that is highly susceptible to fragmentation, erosion, and embolization. Multimodality imaging is required to accurately detect recurrent myxomas by identifying their anatomical features and perfusion; however, each imaging modality has its limitations [5,8,9,13-21]. While 2D TTE and TEE are the preferred techniques for initial assessment, the detection of the type and site of attachment and a detailed evaluation of tumor echotexture and surface characteristics are not always accurate or feasible. Previous reports have demonstrated that 3DE, allowing electronic scanning through unconventional and unrestricted 2D cross-sectional planes likewise an electronic autoptic sectioning, offers additional value in assessing morphological features of cardiac myxomas [8,9,13-18]. MRI is considered the gold standard for diagnosing cardiac tumors and myxomas, enabling not only the detection of intracardiac masses but also the evaluation of various parameters including tissue characterization, edema, iron content, perfusion, enhancement, and fat saturation/suppression [20,21]. However, it also presents some technical limitations and might not always detect anatomical features like tiny stalks [5,13-21]. In the context of cardiac myxoma imaging, 3D TE ECHO, providing detailed

real-time anatomical imaging and unique electronic scanning, may play an emerging role as key adjunctive modality, especially when anatomical clarity is lacking with two-dimensional echocardiography and advanced surgical planning is required [10,11,16,17]. Furthermore, the use of anatomical imaging and an anatomy-based vocabulary, which is better understood by cardiac surgeons and multimodality imagers, positions 3D TE ECHO as the echocardiographic modality that can enhance communication within the Heart Team [10,11]. By bridging the gap between 2D echocardiography and anatomy and adding more detailed information on the morphologic features, its utilization could represent a missing link in myxoma imaging [10-19].

Methods

Study design

This was a retrospective observational study that included patients who had surgery and had a pathological diagnosis of cardiac myxoma. Patients' demographics, symptoms, presence of embolism, imaging performed (2D TTE, 2D TEE, 3D TEE, MRI), surgery, and histological type of myxomas were all studied.

Echocardiography

2D and three-dimensional (3D) transthoracic and transesophageal echocardiography (TEE) data were reported. iE33, EPIC 7C and EPIC CVS 3D system (Philips Medical Systems, Andover, MA, USA) and GE E90, E95 echocardiographic machines equipped with 2D and 3D transesophageal echocardiographic imaging have been used. All images were stored digitally and were offline reviewed on the machine and on Qlabs software (Philips Medical Systems) and EchoPAC (GE HealthCare, Chicago, IL, USA). Electronic 2D scanning of the 3D anatomical and surgical view has been performed to detect the size, location of the tumor, the presence or absence of a stalk, the smoothness of the surface (smooth vs lobulated), and the presence or absence of papillary excrescences, echotexture described as similar or different to the myocardium (hypoechogenic or hyperechogenic) and as homogenous or heterogeneous according to the absence or presence of areas with different echotexture.

Magnetic resonance

Cine steady-state free procession, first pass perfusion and late gadolinium enhancement (LGE) will be reviewed and analyzed. T1 weighted, T2 weighted and T2 fat saturated sequences acquired in two planes orientated will be examined. Steady-state free procession (SSFP) cine imaging sequences, acquired in standard cardiac imaging planes, provide an accurate assessment of the location, attachment site and functional impact of myxomas. On cine SSFP sequences, myxomas typically appear hyperintense compared with normal myocardium and hypointense compared with the blood pool. Cine SSFP imaging is of particular value in the functional assessment of atrial myxomas, as lesions here can be highly mobile.

Results

We have retrospectively collected 17 myxomas in 13 patients, 9 female, mean age 40 range 18-71 years (Table 1).

Case #1

A 42-year-old female with a history of diabetes mellitus, hypertension, and a prior stroke, was admitted to the hospital due to symptoms suggestive of a stroke. Subsequent brain imaging through both CT and MRI indicated findings consistent with chronic ischemic injury. In the process of investigating the stroke, comprehensive cardiac evaluations were conducted, including TTE revealed the presence of a mass attached to the left atrium attached to the interatrial septum (IAS) the mass size was 18x21 mm. 2D 3D TEE showed large mobile mass seen in the left atrium measured at least 18x21 mm attached to the IAS, not causing significant obstruction to flow across the mitral valve. The mass was surgically resected, and the pathology showed mass to had solid characteristics, organized in cord-like formations with no vascular structures within the mass.

Case #2

A 57-year-old female hypertensive, diabetic, with a history of previous cerebrovascular accident (CVA), *in sinus* rhythm, underwent a transthoracic echocardiography (TTE) to detect the source of embolism following a newly diagnosed CVA. The exam showed a large mobile mass in the left atrium (size 1.7x3 cm), with irregular shape and borders and with an nonhomogeneous echo-structure. The mass seemed to originate from the right inferior pulmonary vein (RIPV) or from the basal IAS. Cardiac magnetic resonance (CMR) showed a

mass in the LA, isointense on T1 images and with heterogeneous enhancement on late gadolinium. It was unable to identify a peduncle or clearly identify the site of attachment. No opacification of the mass was found by angiography. Cardiac CT scan also found a mass in the LA close to the RIPV but again it failed to characterize its attachment. A TEE was then performed. It demonstrated the presence of a mobile mass, protruding into the RIPV, without being able to correctly identify its origin. Careful assessment did not reveal other masses in LA and LA appendage. Further 3D acquisition was performed. By using 2D cutting planes on the 3D volume, the mass was sectioned in the different planes by the blue plane of section we were able to identify the attachment of the mass as a tiny peduncle to the atrial floor at the base of the IAS close to the opening of RIPV. Surgical resection revealed reddish jelly mass (size 3x3 cm) with soft consistency attached to the atrial floor at the base of the IAS close to the RIPV. Pathological evaluation confirmed the diagnosis of myxoma [16].

Case #3

A 53-year-old male with a prior history of colorectal cancer underwent a routine abdominal CT scan to monitor his condition's progression. Unexpectedly, the scan revealed a mass in the left atrium near the mitral valve. Further 2D TTE showed a mass attached via a pedicle to the interatrial septum in the region of fossa ovalis sized 1.5 x 4.2 cm. 2D 3D TEE confirmed the TTE findings and imaged the mass to be ovoid, measuring 23x20 mm, attached to the IAS by a thick peduncle attachment. A cardiac MRI was subsequently demonstrated a mass lesion sized at 2.3x1.8 cm. attached to the atrial septum by a pedicle; the mass displayed increased signal intensity in short tau inversion recovery (STIR) and T1 sequences. contrast-enhanced sequences showed limited enhancement during perfusion and delayed phases. Pathology found a solid type myxoma.

Case #4

A 31-year-old female referred from local hospital with a diagnosis of left atrial mass for further evaluation. 3D/2D TTE showed sessile attachment to the lateral left atrial wall that was confirmed at 2D TEE (Figure 1). The atrial mass was large size and has irregular surface, fimbriated (fluffy appearance). At surgery a gelatinous, very fragile mass attached to the roof of LA matching the imaging features was found and resected. Pathology examination found a papillary type myxoma.

Case# 5

A 33-year-old female who underwent left atrial myxoma resection was found to have on a follow up TTE a large multilobular mass in the right atrium (RA). The RA mass was partially protruding into the tricuspid valve during diastole with no significant obstruction to flow. It was not possible to correctly detect the type of the insertion of the tumor; no other masses were found. The patient was not aware of other occurrences of cardiac myxomas in family members. Further 2D TEE showed two multi-lobulated masses in RA: one bigger (measuring around 4 x 3 cm , difficult to correctly size for its asymmetric morphology) attached by a peduncle to the superior lateral RA wall and one smaller attached by a stalk to the inferior RA wall; a remnant likely a suture was seen on the right side of the fossa ovalis; two additional masses were detected in the left atrium: - a small (size 0.7 for 1,4 cm) sessile mass on the left atrial (LA) side of the interatrial septum (IAS) close to the scar of the previous surgery; - a small sessile (size 0.6x0.8 cm) mass attached to the mitral annulus close to the posteromedial commissure and P3 scallop of the posterior leaflet of the mitral valve. 3D TEE allowed an anatomical imaging able to identify two pedunculated right atrial masses and three sessile LA masses: - one on the left side of the interatrial septum close to the previous resection area; - one at the opening of the LAA (left atrial appendage) and one on the mitral annulus in the area of the posterior commissure of mitral valve. MRI multifunctional assessment CINE , tissue characterization with T2 weighted edema imaging with fat saturation and first pass Gadolinium perfusion imaging and late enhancement imaging identified and showed perfusion of - two masses in the RA with the pedicles - one mass on the LA side of interatrial septum; - one mass on the mitral annulus close to mitral valve posterior commissure; however, it was not able to detect the small mass close to the LA appendage even after careful review by an expert reader. The patient underwent reoperation through a biatrial approach ; two lesions were found in the right atrium ; one multilobular with two consistencies, one solid and one myxomatous, both connected by a thick pedicle to the right atrial wall superiorly and laterally; this one was resected with the underlying attachment to the right atrium ; another separate lesion with a separate pedicle and attachment to the right atrial wall more inferiorly was also detected; it was also resected with the adjoining atrial tissue. Three lesions were found in the left atrium; one, about 1 cm of diameter, close to the scar for the last surgery and also other two, smaller in size; one close to the opening of the left atrial appendage and one close to the posterior commissure of the mitral valve. The mitral valve was slightly involved during the resection of the lesion from the valvular annulus and was repaired by 4-0 Prolene sutures. Five specimens were sent to pathology; all of them, upon histopathologic study, were consistent with benign

cardiac myxoma. No major clinical criteria suggestive of Carney Syndrome (skin, conjunctiva and lips lentigines, subclinical hypercortisolism and nodular thyroid changes) except than cardiac myxoma and no mutations of *PRKAR1A* gene were found. After 18 months follow up, no recurrences have been detected [17].

Case #6

A 65-year-old female patient with a medical history of diabetes, hypertension, and a previous myocardial infarction, presented to a local hospital with symptoms of pneumonia. During her work up, she was incidentally found a mass within the left atrium by echocardiography. For this reason, she was referred to our center. 2D TTE confirmed the presence of the left atrial mass, however it was not possible to clearly to identify the attachment. A subsequent 2D 3D TEE was able to demonstrate the sessile attachment to the interatrial septum (IAS). Surgical resection done confirmed the echo findings. Pathology found the mass be a solid myxoma.

Case #7

A 46-year-old female, presented to the emergency department with a history of exertional dyspnea, accompanied by palpitations and chest tightness. 2D TTE revealed a 60x33 mm mass with two distinct hypoechoic regions, suggestive of necrotic and hemorrhagic areas, highly mobile and protruding through the mitral valve into the left ventricle, causing significant obstruction to the flow (Figure 2). 2D, 3D TEE showed the huge atrial mass be pedunculated and attached to the interatrial septum with central large hypoechogenic area with cystic appearance likely central hemorrhage. The patient underwent surgical removal of 4.5 cm mass which was diagnosed at pathology to be a solid myxoma (Figure 2).

Case #8

A 47-year-old male presented with back pain and bradycardia. 2D TTE revealed a left atrial mass, but attachment was unclear. 2D 3D TEE confirmed the mass as pedunculated, attached to the interatrial septum. Cardiac MRI described a 4.2x2.5x 2.6 cm mobile lobulated mass in the left atrium, arising above the fossa ovalis, in contact with the mitral valve but not protruding. It showed varied intensities on T1 and STIR sequences, with central hypervascularity and peripheral enhancement post-contrast, possibly due to a fibrovascular core. Surgical excision yielded a 3 x 4 cm mass attached to the septum. Pathology highlighted a smooth pedunculated surface with hemorrhagic nodules.

Case #9

A 71-year-old female with a history of aortic stenosis, diabetes mellitus, and chronic kidney disease and severe aortic stenosis was scheduled for aortic valve replacement. At preoperative 2D TTE, no LA mass was reported. Unexpectedly, pre-operative 3D TEE revealed a 19x12 mm sessile mass in the left atrium attached to the interatrial septum. During surgery, the atrial mass was excised, the aortic valve was replaced, and coronary artery bypass was performed. Gross examination of the mass demonstrated gray-tan fibrous tissue, and pathology identified a myxoid lesion with fibrous stroma.

Case #10

A 39-year-old male presented with diarrhea and abdominal pain. Abdominal CT identified ulcerative colitis and an incidental hypodense, sessile, lobulated mass adhering to the left atrium's inferior wall. Subsequent 2D TTE revealed a 14x24 mm mobile mass on the interatrial septum. 2D 3D TEE imaged a mass with heterogeneous texture, well-defined borders, with on the top fimbriated edges, attached to the atrial wall. Before surgery, the patient exhibited right-sided weakness, slurred speech, and heaviness. Brain CT indicated an embolic stroke. Surgical excision revealed a 3.5x3.5 cm thrombosed mass on the left atrium's anterolateral wall. Grossly, the mass was a brown-tan and firm. Pathology described solid myxoma arranged in cords with vessels.

Case #11

A 19-year-old female with a history of double outlet right ventricle, dextro-transposition of great vessels, hypoplastic right ventricle, large inlet ventricular septal defect, and overriding tricuspid valve underwent Blalock-Taussig shunt, Glenn shunt, and Fontan procedures. During her annual 2D TTE, a 2x2 cm mobile mass with a short tick pedicle was identified in the right ventricular outflow tract (RVOT) below the aortic valve without sub-aortic obstruction. 2D 3D TEE characterized the mass as a rounded, with delineated borders, attached by a short tick pedicle in the RVOT below the aortic valve, heterogeneous without causing RVOT obstruction (Figure 3). Cardiac MRI confirmed the mass attached to the RVOT below the aortic valve with LGE. Surgical excision yielded soft red tissue. Pathology confirmed the mass as a solid myxoma, vasoformative subtype.

Case #12

An 18-year-old male who already underwent 2 surgical resections of myxomas, one in the left atrium (4 years before) and a second in the right atrium (3 years before), with heterozygous PRKAR1A gene mutation, indicative of Carney complex, was found to have by TTE a recurrent right atrial mass, attached to the IAS (Figure 4). 2D and 3D TEE detected a large mobile, with well delineated margins and heterogenous mass attached to the RA wall just anterior to the mouth of the IVC, measuring ~ 4x3 cm in diameter and partially protruding into the TV inflow and partially obstructing the inflow of the coronary sinus. No obstruction to IVC, SVC or TV inflow. CMR reported a 2.7 x 3.7 x 4.6 cm lobulated RA mass, contiguous with the tricuspid valve's posterior leaflet, partially extending to the atrio-caval junction and mildly intruding the IVC without causing obstruction. Imaging displayed intermediate T1, and high T2 and STIR signal intensities. Perfusion images exhibited mild heterogeneous enhancement. Surgical excision revealed a red-tan, multinodular, hemorrhagic tissue/mass coated in gelatinous material. Histopathology identified a solid myxoma with ectatic vessels, fibrin, stellate cells in a myxoid matrix, multinucleated giant cells, and hemosiderin-laden macrophages. The patient remained recurrence-free after 3-year-follow up.

Case #13

A 48-year-old female known to have HTN incidentally diagnosed with LA mass during evaluation of breast cyst by CT scan. TTE imaged a rounded shaped, with smooth surface, homogeneous, large mass (1.9x1.6 cm) attached to fossa ovalis whose type of attachment was not visualized. 3D/2D TEE were able to better assess the morphological feature and attachment by a peduncle to the fossa ovalis; cardiac MRI showed mobile mass attached to fossa ovalis with LGE. Surgical excision done grossly showed: reddish ovoid mass smooth surface attached by large stump to IAS, pathology confirmed solid tumor.

Discussion

Our series demonstrated a wide and unusual anatomical spectrum of cardiac myxomas. The classical morphology of the myxoma (mobile with well delineated margins attached by a stalk to the interatrial septum) was present in the minority of cases, with most of them being sessile. We have 17 myxomas in 13 patients with a wide variety of origin in different areas of the RA, LA, IAS, LAA, MV and RVOT. The rarer and unusual locations were right ventricular outflow tract (RVOT) in a patient with double outlet right ventricle and dextro-transposition of great vessels, LAA and mitral valve. The texture showed a wide variety (homogeneous myocardial

like, heterogeneous with hyperechogenic areas suggestive of calcifications or hypoechoic areas consistent with intratumoral hemorrhage. The heterogeneousity was better visualized by 3D electronic sectioning. In one patient a huge size myxoma exhibited a cystic appearance with a central large hypoechogenic area found at surgery and pathology be an intratumoral hemorrhage. The size ranged from small to huge dimensions. 2D TEE showed to be able to visualize the anatomical features better than TTE in particular dealing with the type of attachment. 3D TEE confirmed all the findings of 2D TTE but allowed for more detailed assessment of the mass' anatomical features. In all the myxomas 3D TEE was able to correctly identify the peduncle that was not seen in 4 cases by 2D TEE and two small recurrent small myxoma were not visualized by 2D TEE and by MRI. In 2 patients myxomas were papillary, one of them had embolism, attachments were atypical for location and type (1 tiny peduncle on the base of IAS close to RIPV and the other sessile in the roof of the LA) and the texture was homogeneous with irregular fimbriated margins, one with fluffy appearance. 1 patient with solid myxoma experienced embolism and at surgery it was found to have a clot attached on the mobile side. Two patients had recurrence; the first without major clinical criteria suggestive of Carney syndrome (skin, conjunctiva and lips lentigines, subclinical hypercortisolism and nodular thyroid changes) except than cardiac myxoma and no mutations of *PRKAR1A* gene. Unusual was the histology that revealed a papillary type in the first episode and a solid type with 5 myxomas in the recurrence. In the second case genetic testing revealed a heterozygous *PRKAR1A* gene mutation, indicative of Carney complex associated also with a skin fibromyxoma. Even though echo has an excellent sensitivity for cardiac myxomas diagnosis however the specificity is still modest due to a wide differential diagnosis [1-9]. MRI has a key role in cardiac tumor imaging pathway and it is considered the gold standard for diagnosing cardiac tumors and myxomas allowing not only the detection of the morphologic features of the intracardiac masses but also the evaluation of various parameters including tissue characterization, edema, iron content, perfusion, enhancement, and fat saturation/suppression. However, it also presents some technical limitations and might not always detect anatomical some features like tiny stalks [16,17]. In our series it was able to clearly reveal the anatomical characteristics. In only one case it was not able to detect two small myxomas likely due to the small size and the unusual location [17].

The differential diagnosis is challenging because the myxomas can be misdiagnosed with other cardiac tumors in particular with fibroelastomas [5], hemangiomas [22] where the MRI finding are similar to a myxoma with vascular neoformation as in two of our cases and also clot particularly in unusual location [22] or tuberculoma [23).

In the context of cardiac myxoma imaging, 3D TE ECHO, providing detailed real-time anatomical imaging and unique electronic scanning, may play an emerging role as key adjunctive modality, especially when anatomical clarity is lacking with two-dimensional echocardiography and advanced surgical planning is required [10-19]. Furthermore, the use of anatomical imaging and an anatomy-based vocabulary, which is better understood by cardiac surgeons and multimodality imagers, positions 3D TE ECHO as the echocardiographic modality that can enhance communication within the Heart Team [10,11]. By bridging the gap between 2D echocardiography and anatomy and adding more detailed information on the morphologic features, its utilization could represent a missing link in myxoma imaging [10-19].

Conclusions

Our study showed that myxomas has a wide anatomical spectrum beyond the typical feature making the diagnosis challenging in the clinical arena. A detailed multimodality imaging of the anatomical features is paramount in the differential diagnosis among cardiac masses and the histological types of the myxomas. 3D TEE has shown to be a valuable additional imaging technique able to add important morphologic information useful in clinical decision making and in surgical planning.

References

1. Bjessmo S, Ivert T. Cardiac myxoma: 40 years' experience in 63 patients. Ann Thorac Surg 1997;63:697-700.
2. Centofanti P, Di Rosa E, Deorsola L, et al. Primary cardiac tumors: early and late results of surgical treatment in 91 patients. Ann Thorac Surg 1999;68:1236-41.
3. Poterucha TJ, Kochav J, O'Connor DS, Rosner GF. Cardiac tumors: clinical presentation, diagnosis and management. Curr Treat Opt Oncol 2019;20:66.
4. Tyebally S, Chen D, Bhattacharyya S, et al. Cardiac tumors: JACC CardioOncology state-of-the-art review. JACC CardioOncol 2020;2:293-311.
5. El Sabbagh AD, Al-Hijji MA, Thaden JJ, et al. Cardiac myxoma: the great mimicker. JACC Cardiovasc Imaging 2017;10:203-6.
6. Kalçık M, Bayam E, Güner A, et al. Evaluation of the potential predictors of embolism in patients with left atrial myxoma. Echocardiography 2019;36:837-43.
7. Koritnik P, Pavsic N, Bervar M, Prokselj K. Echocardiographic characteristics of cardiac myxoma. Eur Heart J 2021;42:ehab724.0146.

8. Mankad R, Herrmann J. Cardiac tumors: echo assessment. Echo Res Pract 2016;3:R65-R77.
9. Parato VM, Nocco S, Alunni G, et al. Imaging of cardiac masses: an updated overview. J Cardiovasc Echogr 2022;32:65-75.
10. Lang RM, Addetia K, Narang A, Mor-Avi V. 3-dimensional echocardiography: latest developments and future directions. JACC Cardiovasc Imaging 2018;11:1854-78.
11. Faletra FF, Agricola E, Flachskampf FA, et al. Three-dimensional transoesophageal echocardiography: how to use and when to use - a clinical consensus statement from the European Association of Cardiovascular Imaging of the European Society of Cardiology. Eur Heart J Cardiovasc Imaging 2023;24:e119-e197.
12. Galzerano D, Kinsara AJ, Di Michele S, et al. Three dimensional transesophageal echocardiography: a missing link in infective endocarditis imaging? Int J Cardiovasc Imaging 2020;36:403-13.
13. Khairnar P, Hsiung MC, Mishra S, et al. The ability of live three-dimensional transesophageal echocardiography to evaluate the attachment site of intracardiac tumors. Echocardiography 2011;28:1041-5.
14. Tolstrup K, Shiota T, Gurudevan S, et al. Left atrial myxomas: correlation of two-dimensional and live three-dimensional transesophageal echocardiography with the clinical and pathologic findings. J Am Soc Echocardiogr 2011;24:618-24.
15. Zaragoza-Macias E, Chen MA, Gill EA. Real time three-dimensional echocardiography evaluation of intracardiac masses. Echocardiography 2012;29:207-19.
16. Galzerano D, Pragliola C, Al Admawi M, et al. The role of 3D echocardiographic imaging in the differential diagnosis of an atypical left atrial myxoma. Monaldi for Chest Dis 2018;88:906.
17. Al Sergani R, Alamr B, Al Admawi M, et al. Three dimensional echocardiographic imaging of multiple recurrent myxomas. Monaldi for Chest Dis 2020;90:1188.
18. Khairnar P1, Hsiung MC, Mishra S et al. The ability of live three-dimensional transesophageal echocardiography to evaluate the attachment site of intracardiac tumors. Echocardiography 2011;28:1041-5.
19. Espinola-Zavaleta N, Lozoya-Del Rosal JJ, Colin-Lizalde L, Lupi-Herrera E. Left atrial cardiac myxoma. Two unusual cases studied by 3D echocardiography. BMJ Case Rep 2014;2014:bcr2014205938.
20. Abbas A, Garfath-Cox KAG, Brown IW, et al. Cardiac MR assessment of cardiac myxomas Br J Radiol 2015; 88:1045.

21. Basso C, Buser PT, Rizzo S, et al. Benign cardiac tumors. In: V. Ferrari, Editor. EACVI Textbook of Cardiovascular Magnetic Resonance. Oxford, Oxford University Press; 2018. p. 469-73.
22. Galzerano D, Eltayeb A, Alamri S, et al. A ping pong ball in the left ventricle. J Cardiothorac Vasc Anesth 2023;37:2153-6.
23. Alamri F, Eltayeb A, Hamad A, et al. A native mitral valve mass beyond imagination. Monaldi Arch Chest Dis 2023. Online Ahead of Print.
24. Pergola V, Al-Admawi M, Fadel B, Di Salvo G. An unusual cardiac mass: echocardiography, computed tomography, and magnetic resonance imaging. J Cardiol Cases 2016;13:143-5.

Figure 1. Case #4. A) TTE image showing 2-chamber apical view with LA myxoma. B) 3D-TEE volume sectioned at different levels showing left atrial myxoma. C,D) Histological examination showing 4 acid-mucopolysaccharide-rich myxoid matrix with polygonal stromal cells scattered throughout papillary myxoma with single cell predominant subtype; the single myxoid cells were scattered.

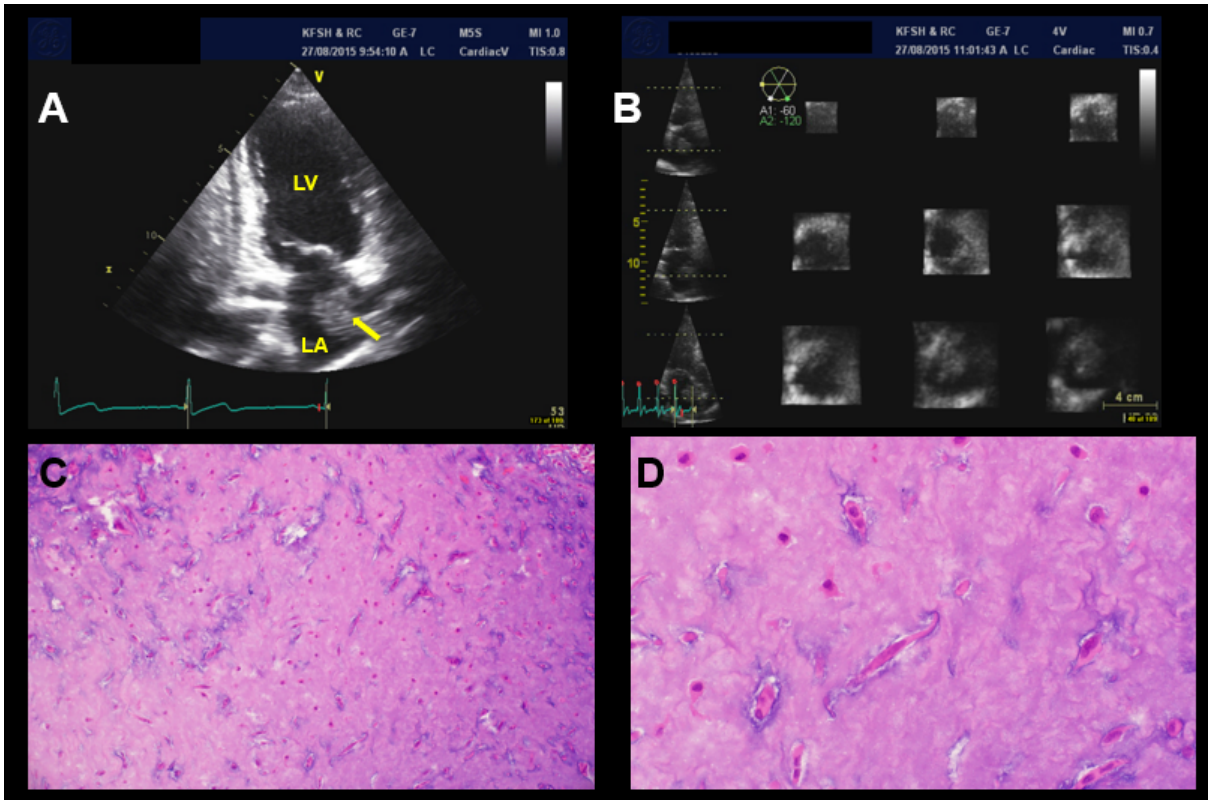

Figure 2. Case #7. A) PLAX view of TTE showing LA mass with ghost appearance obstructing mitral inflow. B) TEE with mid esophageal long axis view at 130 degrees at diastole showing the mass prolapsing through mitral valve. C) Mid-esophageal five-chamber view with the mass in LA attached to IAS by stalk (yellow arrow). D) TEE with two chamber view at 90 degrees with color doppler at systole showing MR directed posteriorly around the mass and 3D TEE image showing the mass interfering with mitral valve closure as possible mechanism of the MR (F). PLAX, para-sternal long axis view; TTE, trans-thoracic echocardiography; TEE, trans-esophageal echocardiography; LA, left atrium; LV, left ventricle; IAS, inter-atrial septum; MR, mitral regurgitation.

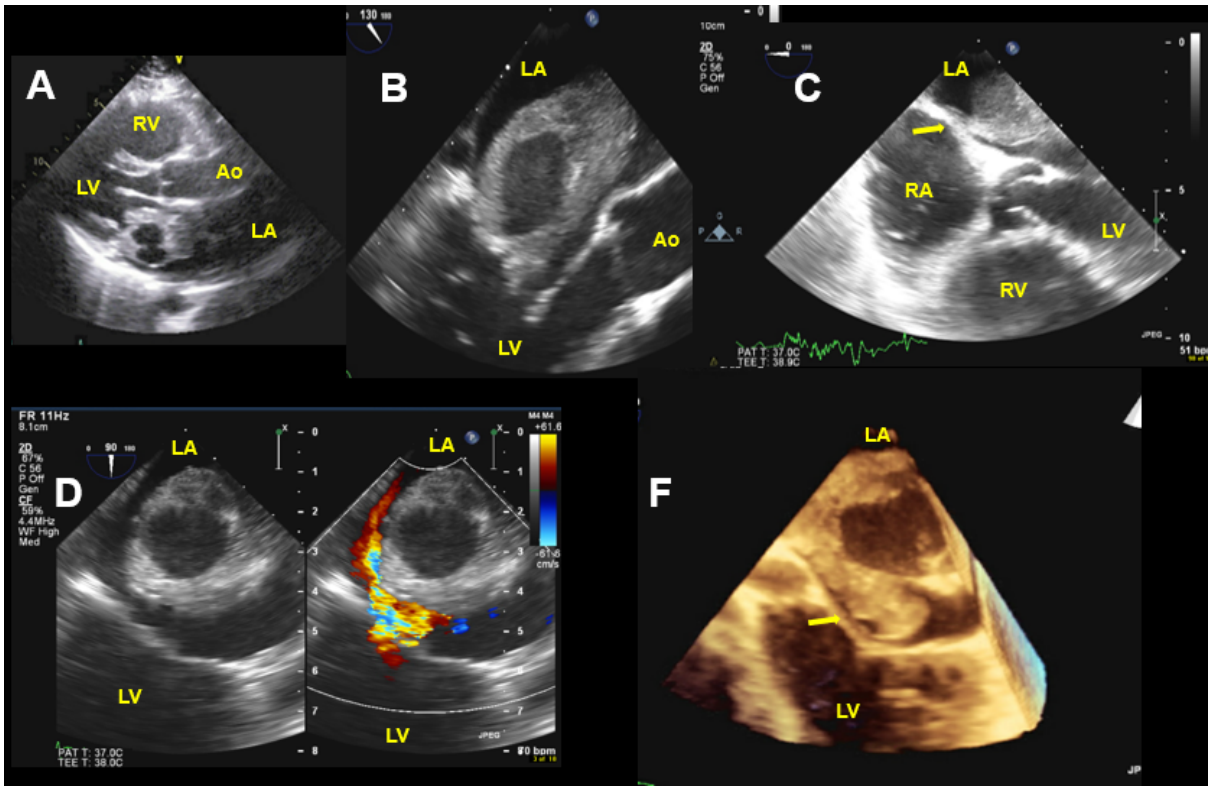

Figure 3. Case #11. A) TEE showing mass attached to the anterior RVOT just below the aortic valve. B) 2-dimensional cross-sectional views on TEE 3D volume showing the attachment to the RVOT (yellow arrow). C) steady-state free precession (SSFP) MRI of RVOT with mass seen below AV (end-diastole and systole). D) Acid-mucopolysaccharide-rich myxoid matrix with polygonal stromal cells; solid mixoma vasoformative subtype. TEE, transesophageal echocardiography; RVOT, right ventricular outflow tract; AV, aortic valve.

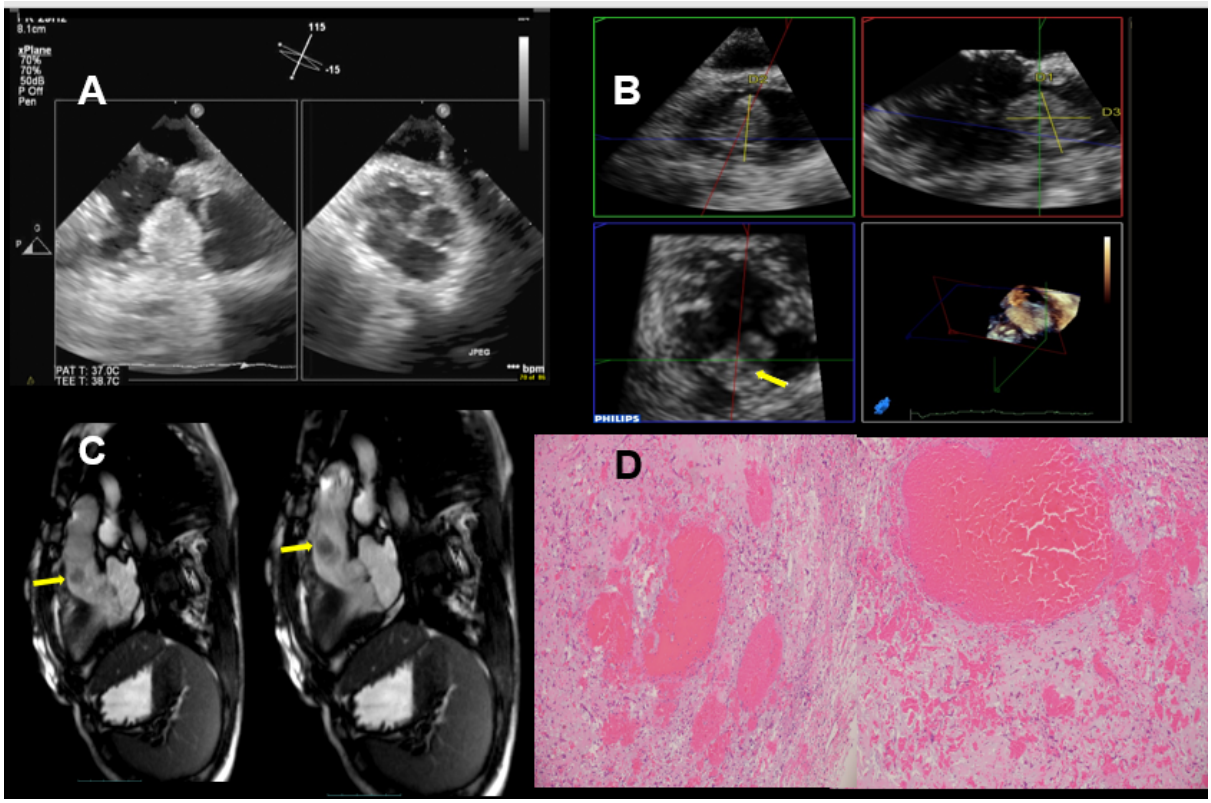

Figure 4. Case #12. A,B) TTE diastole and systole; large atrial RA mass that seems attached to the IAS protruding into TV during diastole. C) 2D TEE RA mass attached to the atrial wall close to the IVC opening. D) 3D TEE; enface view of the RA mass attached to the atrial wall close to the opening of IVC .

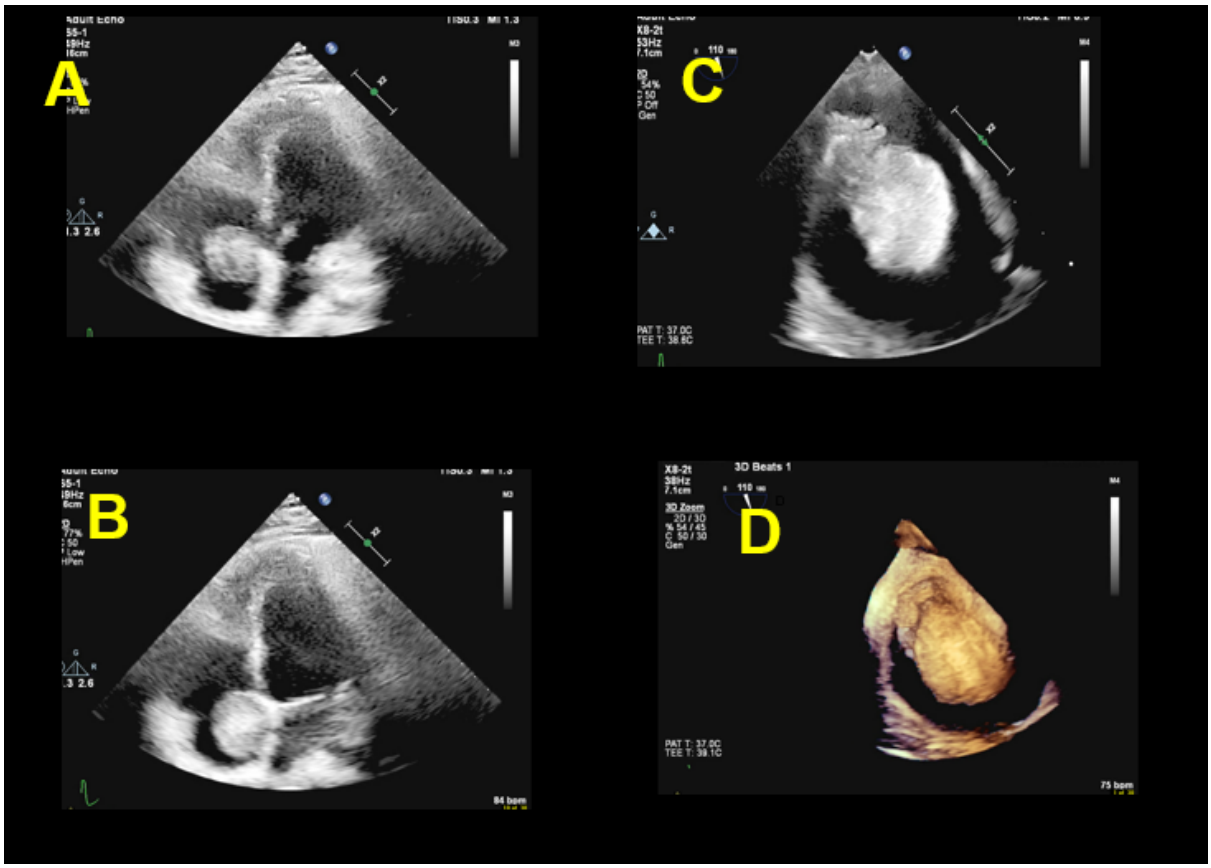

Figure 5. Case #13. A) TTE: rounded shaped, with smooth surface, homogeneous, large mass (1.9x1.6 cm) attached to fossa ovalis whose type of attachment was not visualized. B) 2D TEE X plane showing a round large mass (1.9x1.6 cm) attached to fossa ovalis by a thick stalk. C) Cardiac MRI showed mobile mass attached to fossa ovalis with LGE. D) Intraoperative picture: reddish ovoid mass smooth surface attached by large stump to IAS. E) Grossy specimen. CMR, cardiac magnetic resonance; TEE, trans-esophageal echocardiography; MYX, myxoma; LV, left ventricle; LA, left atrium; RV, right ventricle; RIPV, right inferior pulmonary vein; IAS, inter-atrial septum.

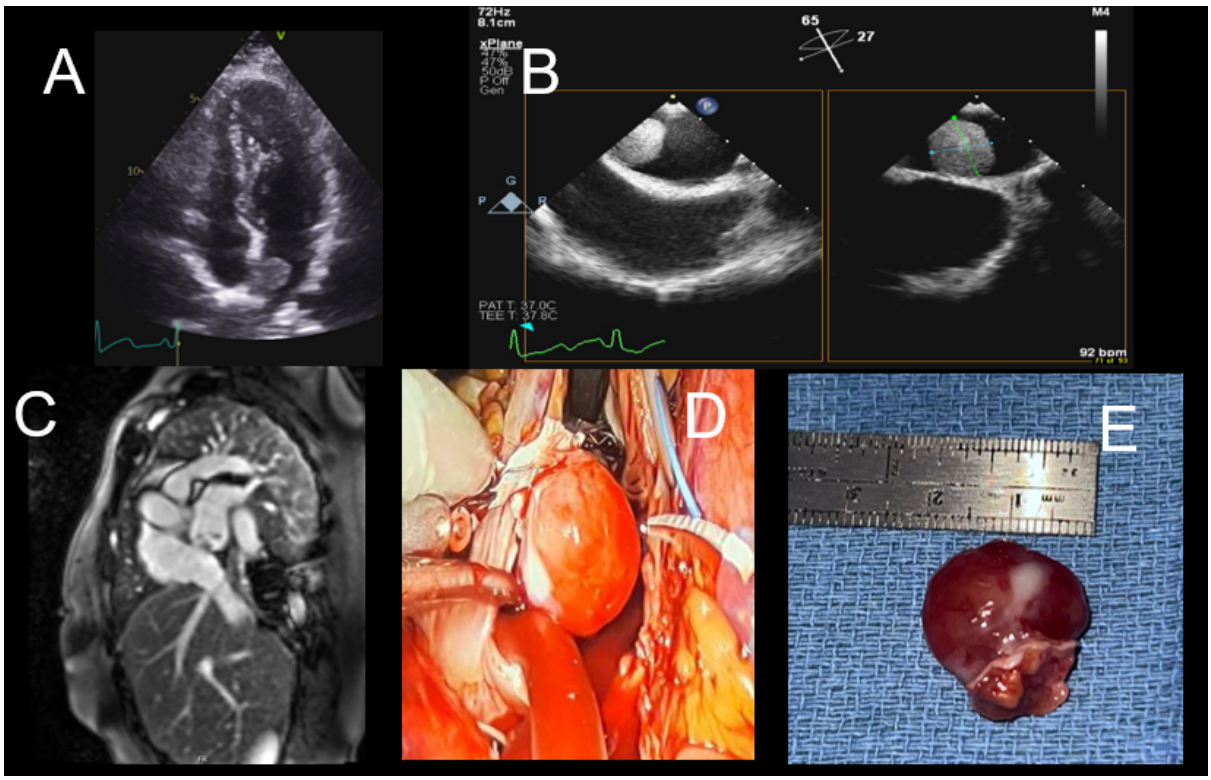

Table 1. Data and characteristics of the study population.

Case	Age/Gender	Symptoms	Echo findings 2D TTE, 2D/3D TEE.	Histology
1	42/F	Yes (Brain infarcts)	2D TTE: Large mobile mass seen in the left atrium measured at least 1.8x2.1 cm attached to the IAS, not causing significant obstruction to flow across the mitral valve. 2D 3D TEE: pedunculated mass attached to the interatrial septum.	Solid
2	57/F	Yes (Brain infarcts)	2D TTE: mobile mass in the left atrium (size1.7x3cm), with irregular shape with an nonhomogeneous echotexture. The mass seemed to originate from the right inferior pulmonary vein (RIPV) or from the basal IAS. 3D TEE: Attached by a peduncle to the inferior atrial septum near to the opening of right inferior pulmonary vein.	Papillary
3	53/M	No	2D TTE: The mass is attached via a pedicle to the interatrial septum in the region of fossa ovalis. (1.5 x 4.2 cm) 2D 3D TEE: Large mass attached to interatrial septum on the left atrial side more anteriorly just behind the aortic valve.	Solid
4	31/F	Yes (Chest pain)	3D/2D TTE: sessile attachment to the lateral atrial wall. The atrial mass is large and has irregular surface, fimbriated (fluffy appearance).	Papillary
5	33/F	No	2D TTE: Multilobulated masses seen in RA. Septal attachment could not be confirmed but it is likely attached to the septal. 3D TEE: Multi-lobulated mass seen in the right atrium that seems attached to the interatrial septum close to svc and aorta; at the same level of the interatrial septum there is another small mass on left atrial side ;; another small mass seen on the close to the opening of LAA; small mass attached close to the posteromedial commissure and P3 scallop of the mitral	Solid

			valve.The RA mass partially protrudes through tricuspid valve during diastole with no significant obstruction to flow.2D	
6	65/F	No	2D TTE: regular border mass is arising from the atrial septum. (Size 2.1x4 cm). 2D 3D TEE: Sessile attachment to the interatrial septum (IAS). With some area of Heterogeneity with regular smooth surface. Size 2.2 x 4.2 cm	Solid
7	46/F	Yes (SOB/ palpitations)	2D TTE: Large and highly mobile mass in the LA, attached to the interatrial septum at the fossa ovale; the mass measures ~ 6 x 3.3 cm and protrudes across the MV in diastole into the LV inflow causing severe obstruction to flow. Two large central hypoechogenic areas noted within the mass may represent central necrosis. 2D 3D TEE: huge mass, pedunculated ,attached to the interatrial septum. size 60 mm x 33 mm	Solid
8	46/M	No	2D TTE: pedunculated, attached to the interatrial septum. 2D TEE pedunculated, attached to the interatrial septum	Solid
9	71/F	Severe aortic stenosis	2D TTE: no Mass by TTE. 3D TEE: Sessile Mass attached to the left side of fossa ovalis (size 1.9 x 1.2 cm) with irregular shape and soft echo structure.	Solid
10	39/M	No	2D TTE: Mobile mass 14x24 mm attached to the interatrial septum. 2D 3D TEE: mass with heterogeneous texture, well-defined borders, with on the top fimbriated edges, attached to the atrial wall	Solid
11	19/F	No	2D TTE: Large rounded mobile mass (2x2 cm) with a short thick pedicle just below aortic valve but no sub-aortic obstruction. 2D 3D TEE Large rounded mobile mass with a short thick pedicle attached to the RVOT just below aortic valve	Solid

12	18/M	No	2D TTE: Large RA myxoma measuring 3.5 x 3.0 cm attached to the IAS with no significant obstruction. 2D 3D TEE. a large mobile, with well delineated margins and heterogenous mass attached to the RA wall just anterior to the mouth of the IVC, measuring ~ 4 cm x 3 cm in diameter and partially protruding into the TV inflow and partially obstructing the inflow of the coronary sinus. No obstruction to IVC, SVC or TV inflow.	Solid
13	48/F	No	2D TTE: Round Large Mass (1.9 x 1.6 cm) attached to fossa ovalis, smooth surface homogeneous likely attached by a peduncle not seen clearly by TTE. 2D 3D TEE: Round Large sessile Mass (1.9 x 1.6 cm) attached to fossa ovalis.	Solid